Quality control of gold nanoparticles as pharmaceutical ingredients

Arnaud Pallotta, Ariane Boudier, Benjamin Creusot, Emilie Brun, Cécile Sicard-Roselli, Rana Bazzi, Stéphane G. Roux, Igor Clarot

Quality Control of Gold Nanoparticles as Pharmaceutical Ingredients.

Arnaud Pallotta[1,2], Ariane Boudier[1,2], Benjamin Creusot[1], Emilie Brun[3], Cécile Sicard-Roselli[3], Rana Bazzi[4], Stéphane Roux[4], Igor Clarot[1,2*]

[1]: Université de Lorraine, CITHEFOR, F- 54000 Nancy, France

[2]: Nanocontrol, Nancy, France

[3]: Université Paris Sud, Laboratoire de Chimie Physique, UMR CNRS 8000, F-91405 Orsay, France

[4]: Université de Bourgogne Franche-Comté, Institut UTINAM, UMR 6213 CNRS-UBFC, F-25000 Besançon, France.

*Corresponding author:

Igor Clarot: +33 3 72 74 72 70

igor.clarot@univ-lorraine.fr

Abstract

Nanoparticles are being developed for a wide range of medical applications such as, controlled release, drug delivery systems or imagery, theranostics, implants.... For the moment, there is no legal definition of nanoparticles or nanomaterials for therapeutic use. The specific case of gold nanoparticles is not an exception: their current definition as nanoparticle material does not correspond to classic pharmaceutical ingredients as described in Pharmacopoeias. In this study, more than 30 different batches of citrate stabilized gold nanoparticles (AuNP) were synthesized and analyzed thanks to both classical approaches (UV-Vis spectrophotometry, dynamic light scattering coupled or not to electrophoresis …) and capillary zone electrophoresis (CZE) coupled to diode array detection to assess their purity and impurity profiles. These techniques led to the beginning of defined specifications, a key step for the use of gold nanoparticles as pharmaceutical ingredients. CZE was demonstrated suitable to evaluate a batch-to-batch quality control, to monitor the purification processes and to follow the stability of 18 different batches for 20 days. Finally, commercially available AuNP samples were tested and the results compared to the provided certificates of analysis.

Keywords: Gold nanoparticles, Pharmaceutical ingredient, Capillary electrophoresis, Assay, Impurity profile, Stability

1. Introduction

Since recent years, nanoparticles (NP) development is an extensively growing research field for biomedical applications (D'Mello *et al.*, 2017) especially for cancer diagnosis and treatment (Brigger *et al.*, 2002; Hardie *et al.*, 2016; Pallotta *et al.*, 2019; Rawal and Patel, 2019; Silva *et al.*, 2019; Yi *et al.*, 2016). Several types of NP are under investigation and among the inorganic ones, gold nanoparticles (AuNP) are widely studied and used for numerous applications (Figure 1). Their properties have led to several studies from preclinical to clinical trials. At the moment, eight trials concerning AuNP are set up with different therapeutic targets (such as cancer treatment, type I diabetes, coronary diseases, Parkinson's disease, pulmonary hypertension), half of which implies *in-vivo* use (Table 1).

Table 1 : Clinical Trials using AuNP extracted from https://clinicaltrials.gov/ using on the 2019 19th of March with keyword AuNP. For more information on studies use the identifier number on https://clinicaltrials.gov/.

Identifier	Study Title	Subject Conditions	Use
NCT01436123	Plasmonic Photothermal and Stem Cell Therapy of Atherosclerosis Versus Stenting	Coronary Artery Disease Atherosclerosis	Injection
NCT02837094	Enhanced Epidermal Antigen Specific Immunotherapy Trial -1	Type 1 Diabetes	Intradermal injection
NCT03020017	NU-0129 in Treating Patients With Recurrent Glioblastoma or Gliosarcoma Undergoing Surgery	Gliosarcoma Recurrent Glioblastoma	Intravenous injection
NCT01270139	Plasmonic Nanophotothermal Therapy of Atherosclerosis	Stable Angina|Heart Failure Atherosclerosis Multivessel Coronary Artery Disease	NP on patch
NCT03669224	Effect of Nano Care Gold on Marginal Integrity of Resin Composite	Caries Class II	Surface pre-treatment of the resin by AuNP
NCT02782026	Exhaled Breath Olfactory Signature of Pulmonary Arterial Hypertension	Pulmonary Hypertension	Sensor array with AuNP

NCT01420588	Diagnosis of Gastric Lesions With Na-nose	Stomach Diseases	Sensor array with AuNP
NCT01246336	Exploratory Study Using Nanotechnology to Detect Biomarkers of Parkinson's Disease From Exhaled Breath	Parkinson's Disease Parkinsonism	Sensor array with AuNP

AuNP are biocompatible, easily synthesized and can be functionalized by a wide range of molecules and active substances. Their specific optical properties make them used as biosensors (Aldewachi *et al.*, 2017; Devi *et al.*, 2015; Nie *et al.*, 2014; Shawky *et al.*, 2017) or diagnostic agents (Lu *et al.*, 2012). Thus, they emerge as powerful theranostic platforms (Guo *et al.*, 2017; Singh *et al.*, 2015).

The translation of AuNP from bench to bedside requires to ascertain purity and impurity profiles of the synthesized product. For classical drugs and excipients, profiles are described and reported in Pharmacopoeia (FDA for the USA, EDQM for Europe and PMDA for Japan). However, for AuNP as for all NP, no official consensus exists. Their characterization remains a challenge throughout NP synthesis. Among the numerous available characterization techniques, most focus on physicochemical parameters and allow determining:

- Their size: core size (transmission electronic microscopy (TEM)) or hydrodynamic diameter (Dh) (dynamic light scatting (DLS)).
- Their surface charge (ζ potential): DLS coupled to electrophoresis.
- Their chemical composition: atomic spectroscopies, X-Ray Photoelectron spectroscopy (XPS), Secondary Ion Mass Spectroscopy (SIMS) …

The indicated methodologies are the ones used currently to determine physicochemical parameters of NP (ISO/TS, 2008). But several drawbacks have already been reported in the literature. On the one hand, TEM is a very powerful tool to determine the morphologie and size of a batch of nano-objects (ISO/TR-18196:2016, 2016; Varenne *et al.*, 2016). However, it is always performed on dry samples leading to possible modifications compared to NP in their liquid medium *i.e.* after synthesis or incubation in biological media (hydration and

solvation layers, ligand or protein adsorption...). Cryo-TEM could be used to assess liquid samples (Stewart, 2017) but is not used in routine yet and is usually difficult to access. DLS, on the other hand, allows simple measurements in liquid media. It is low-cost and easy handling (ISO-22412:2017, 2017; ISO/TR-18196:2016, 2016; Varenne *et al.*, 2016). DLS give accurate results as long as monodisperse samples are studied. The hydrodynamic diameter is given assimilating nano-objets to spheres. Data obtained on samples with high polydispersity or interacting with light (such as metallic NP) must be treated with caution (Bhattacharjee, 2016; Varenne *et al.*, 2016). To overcome this drawback, it is possible to associate DLS with a pre-separation step, such as Field Flow Fractionation but it can be biased by the presence of large particles (Clogston *et al.*, 2016). Concerning surface charge, ζ potential is highly dependent on experimental parameters (dispersion medium, salt concentration, pH, instrument parameters …). In addition, ζ potential determination can sometimes be difficult for small particles (< 40 nm) (ISO/TR-18196:2016, 2016; Varenne *et al.*, 2015). Finally, the previously mentioned methods that analyze the chemical composition of NP are often used on dry samples which can be responsible of artifacts (Muneshwar and Cadien, 2018). Moreover, they require complex handling, are not readily accessible and thus are not used in routine.

Additionally, these different approaches do not give any information on the impurity profile of the sample. Separative methods have been previously applied to characterize NP: liquid chromatography coupled to mass spectrometry (LC-MS) (Mishra and Mukhopadhyay, 2019), size exclusion chromatography (SEC) (Duesberg *et al.*, 1998), Field Flow Fractionation (Zattoni *et al.*, 2009). Capillary zone electrophoresis (CZE) is also suitable for this purpose (Pallotta *et al.*, 2016). AuNP have been separated according to their size (Franze *et al.*, 2017; Pallotta *et al.*, 2016) and shape (Surugau and Urban, 2009) with a high resolution. It has also been used to evaluate the surface chemistry of AuNP and their stability. Thus CZE has been proposed as a method of choice for quality control of inorganic NP (Pallotta *et al.*, 2016).

International Conferences on Harmonization (ICH) is an organization regrouping Pharmacopoeias from all around the world and gives guidelines for Quality and safety of medicines. These recommendations include the definition of precise specifications so that a substance can be declared in conformity with its intended use (ICH Q6A, (ICH-Q6A)). Important specifications are related to the limits imposed for impurities (ICH Q3A(R2), (ICH-Q3A(R2))). Impurities in new substances derived from chemical synthesis may be "organic, inorganic or residual solvents". They result from the synthesis (starting materials, by-products, intermediates, reagents…) or degradation products. For nanoparticles, these definitions must also be applied with certain adjustment: if nanoparticles other than those defined in the specifications exist in the sample, they must also be considered as impurities (populations with different sizes or charges or even aggregates for example). Their assessment and the substance content (assay percentage) are essential for the initial definition of the NP as a pharmaceutical ingredient. For a safety of use, these criteria and in particular the impurity profiles must be evaluated over time to define their stability (*e. g.* a maximum permissible deviation of 5% from the initial content in ICH Q1A(R2) (ICH-Q1A(R2)))

Lately, several reviews and articles have been published concerning the lack of quality control during NP manufacturing process, the complexity to switch from a lab scale to an industrial scale production (Coty and Vauthier, 2018; Gonzalez-Fuenzalida *et al.*, 2019; Pallotta *et al.*, 2019; Stavis *et al.*, 2018) and the need for future standards for the evaluation of nano-ingredients (Gioria *et al.*, 2018; Halamoda-Kenzaoui *et al.*, 2019).

In this study, we focused on gold nanoparticles stabilized by citrate ions (AuNP-Cit) because they are often the basic elements or the synthesis of more complex nano-objects (functionalization by ligands for example). All the batches studied in this work were analyzed using classical methodologies (*i.e.* UV-Vis spectrophotometry, DLS coupled or not to electrophoresis (ζ potential), TEM) and CZE coupled to a diode array detection (DAD) for contents and impurities.

Some batches synthesized from laboratories of the French network GDR Or nano (http://or-nano.insp.upmc.fr) were monitored all along the synthesis process to evaluate purification or centrifugation processes. Eighteen batches were monitored for evaluation of their stability with time. Finally, the methodologies developed were applied to commercial AuNP batches to determine their value as pharmaceutical ingredients. The main objective of this work is to complement traditional techniques for nanoparticle analysis to ascertain their safety of use in the pharmaceutical sector. A higher quality grade can be achieved and would be a major step forward in other sectors such as cosmetics, agri-food or microelectronics.

2. Materials and methods

2.1. Chemicals

All reagents and solvents were of analytical grade and used without further purification. Sodium borohydride, sodium citrate, dithiolated diethylenetriamine pentaacetic acid (DTDTPA), hydroxyethyl piperazineethanesulfonic acid (HEPES) , tetrachloroauric acid trihydrate ($HAuCl_4.3\ H_2O$), potassium tetrachloaurate ($KAuCl_4$), HCl 1.0 M, and NaOH 1.0 M, acetonitrile, trifluoroacetic acid, tannic acid, silver nitrate, sodium borohydride ($NaBH_4$), fuming HCl, Rhodamine B and diisopropyl ether were supplied by Sigma Aldrich. Boric acid and NaOH pellets were purchased from Riedel-de-Haën. Ultrapure water (> 18.2 mΩ.cm) was used for the preparation of all solutions. Commercial AuNP (5 nm core diameter, citrate stabilized) samples were purchased from Nanocomposix and Sigma-Aldrich.

2.2. Citrate stabilized gold nanoparticles synthesis

Citrate stabilized AuNP (AuNP-Cit) were synthesized in aqueous solution as already described (Tournebize, Boudier, Joubert*, et al.*, 2012; Tournebize, Boudier, Sapin-Minet*, et al.*, 2012; Tournebize *et al.*, 2011). Briefly, 1 mL of $AuCl_4^-$ solution (10 mg/mL) was added in 90 mL of water and 2 mL of sodium citrate 55 mM was added. The solution was stirred for 1 min then 1 mL of $NaBH_4$ 19.5 mM was added and the solution was stirred again for 5 min under nitrogen. The resulting suspension was immediately stored in the dark at 4 °C. The final concentration was 90 nM.

Several batches were received from other laboratories with their own labelling. The first batches (from A to D) were not evaluated in this paper. Analyzed batches were called “E, F and G”. For E batch, stock solutions of nanoparticles were prepared as proposed by Slot and Geuze (Slot and Geuze, 1981). AuNP were synthesized by reducing $KAuCl_4$ solutions (125 nM) by a mix of tri-sodium citrate (0.04 % wt final concentration) and tannic acid (0.05 % wt final concentration), previously heated at 60 °C. Purification consisted of three successive centrifugations (195 000 × *g*, 40 min, 4 °C) by replacing each time the supernatant with ultra-pure water.

For F and G batches, a pre-mixing method (Xia *et al.*, 2016), was used. Two mL of $HAuCl_4$ (1 % wt in water) and 170 µL of $AgNO_3$ (0.1 % wt) were mixed. 6 mL (for F) or 2.8 mL (for G) of sodium citrate (1% wt) were added, and water for final volume of 10 mL. After 5 min (for F) or 4 min (for G), the 10 mL solution was dispersed into 190 mL of boiling water and reflux was maintained 30 min.

2.3. Dithiolated Diethylenetriamine Pentaacetic Acid grafted AuNP (AuNP@DTDTPA) synthesis and purification

For a typical preparation of AuNP@DTDTPA, 200 mg (510 µmol) of $HAuCl_4 \bullet 3H_2O$, dissolved in 60 mL of methanol, were placed in a 250 mL round-bottom flask. 256 mg (500 µmol) of DTDTPA in 40 mL of water and 2 mL of acetic acid were added to the gold salt solution under stirring. The mixture turned from yellow to orange. After 5 min, 185 mg (4.89 mmol) of $NaBH_4$ dissolved in 14 mL of water were added to the orange mixture under vigorous stirring at room temperature. When adding $NaBH_4$, the solution became dark brown then a black flocculate formed. The vigorous stirring was maintained for 1 h before adding 5 mL of 1.0 M HCl. After the partial removal of the solvent under reduced pressure and at a maximum of 40°C, the precipitate was recovered on a polymer membrane and washed thoroughly and successively with 0.01 M HCl, water, and diethylether. The resulting precipitate was dried and the recovered black powder (with a yield of up to 200 mg) was dispersed in 10 mL of NaOH with pH 8.0 (raw suspension of AuNP@DTDTPA).

Since these nanoparticles have been developed for image guided radiotherapy, a purification protocol was established in order to prepare a suspension suitable for intravenous injection. The raw suspension of AuNP@DTDTPA was purified by ultrafiltration using Vivaspin® tube (20 mL, molecular weight cut-off (MWCO) 5 kDa). The resulting suspension was diluted with an appropriate volume of a filtered aqueous solution containing NaCl (4 M) and HEPES (135 mM) in order to obtain intravenous use gold nanoparticles suspensions. The pH was then adjusted to 7.4. Before use, the AuNP@DTDTPA suspension was filtered onto a syringe filter with a nylon membrane (pore diameter 0.22 µm).

2.4. AuNP characterization

A UV-Vis spectrophotometer (UV-1800 Shimadzu) was used for spectra recordings and absorbance determinations. The hydrodynamic diameter (Dh) and ζ potential of AuNP were measured at 20 ± 1 °C using a Zetasizer Nano ZS (Malvern Instruments, UK). All values are volume average considering three independent measurements with the same concentration. TEM images were obtained using a Philips CM 200 instrument with a LaB6 cathode operating at 200 kV. Gold NP suspensions were deposited onto a 400 mesh carbon film copper grids. The mean diameter of the gold core of *ca.* 200 individual particles (Dc) obtained from the TEM images was calculated for each AuNP sample. TEM images of the different batches under study were shown in Figure S1 of the Supplementary Material attached file.

2.5. Capillary zone electrophoresis

CZE measurements were carried out using a P/ACE MDQ CE system (Beckman Coulter) equipped with a diode array detector (DAD, λ from 200 to 600 nm) at 25 ± 1 °C and using a 40 cm bare silica capillary (effective length 34 cm). Background electrolyte (BGE) was a 25 mM boric acid/sodium borate buffer pH 8.5 adjusted with 40 % (m/V) NaOH. AuNP detection was performed under 10 kV (normal polarity, cathodic electroosmotic flow (EOF)). Before each injection the capillary was rinsed with NaOH 1.0 M (2 min), ultrapure water (2 min) and BGE (2 min). AuNP were directly injected hydrodynamically (20 mbar for 10 s). EOF was determined using a neutral marker, benzyl alcohol (migration time = 2.06 ± 0.03 min, EOF = 9.1 ± 0.1 × 10^{-4} $cm^2V^{-1}s^{-1}$ (n = 5)). Electrophoretic mobilities (μ_{EP}) of AuNP were calculated using equation (1):

$$\mu_{APP} = \mu_{EP} + \mu_{EOF} \quad (1)$$

where μ_{APP}, μ_{EP} and μ_{EOF} correspond to apparent, electrophoretic and electroosmotic flow mobilities respectively.

Each injection was realized in triplicate and the obtained peaks were identified by their relative migration time (RMT), equation (2):

$$RMT = \frac{T_m}{T_{m\ neutral\ marker}} \quad (2)$$

where T_m is the migration time of the peak of interest and $T_{m\ neutral\ marker}$ is the migration time of the neutral species.

2.6. Gold concentration measurements

Gold concentration was measured according to the method already developed in our laboratory (Pallotta *et al.*, 2018). Briefly, AuNP-Cit samples (400 µL) were mixed with an HCl-NaCl-Br_2 solution (1.0 M, 0.3 M, 0.025 M respectively) for 20 min protected from light in LoBind Eppendorf microtubes (1.5 mL). The mixture was then partially evaporated using a Turbovap (Biotage) at 40 °C under N_2 gas for 20 min. Then, 200 µL of NH_4Cl solution (30 % m/V), 100 µL of 6 M HCl and 100 µL Rhodamine B solution (0.084 µM) were added. The ion-pair formed between $AuCl_4^-$ and Rhodamine B was then extracted in 200 µL of diisopropyl ether. 150 µL of the supernatant (organic phase) were withdrawn, completely evaporated (Turbovap, 40 °C, N_2, 5 min) and the dried residues were dissolved into the mobile phase (acetonitrile/water/trifluoroacetic acid 25/75/0.1 V/V) before injection into the HPLC system.

HPLC analyses were carried out on a SpectraSystem instrument constituted by the following modules: vacuum degasser (SCM1000), quaternary pump (P1000XP), autosampler (AS300) and UV-Visible detector (UV2000). The column was thermostated at 40 °C using a Croco-cit™ (1267) oven. Data acquisition and injection control were performed by the Azur software (version 4.6.0.0, Datalys®). The method used a Nucleosil ®(C18), 150 mm × 4.6 mm, 3 µm particles size and 100 Å porosity. The detector was set at 555 nm and the pump at 1.0 $mL.min^{-1}$. The injection volume was 20 µL.

3. Results and discussion

Defining specifications for pharmaceutical raw materials can be a real challenge. Usually, for new drug substances, interlaboratory studies are a good way to define the imposed limits so that they are accepted and recognized by the manufacturing community. For eventual impurities, monographs have to be designed to cover different impurity profiles as synthesis and/or purification processes used by manufacturers could be different. Impurity specifications have also to be defined for specified impurities with individual acceptance criteria and include a limit of the total impurity accepted. Those limits derive directly from qualification data from producers and are submitted to the competent authorities. In this study, all indicated specifications are based on the numerous syntheses carried out in our laboratory and correspond to limits defined specifically for "simple" gold citrate nanoparticles of defined size (5 nm). In order to confer the grade of pharmaceutical ingredient to nanoparticles, a similar approach must be used for all type of nanoparticles (characterization of charge, size, functionalization…) that will be used for biomedical applications.

3.1. Synthesis and purification processes evaluation

As potential pharmaceutical products, AuNP require a strict control. In a previous work of our laboratory, some specifications were defined to perform quality control of day-to-day AuNP-Cit synthesis (Pallotta *et al.*, 2016). As defined by ICH Q6A (ICH-Q6A): "A specification is defined as a list of tests, references to analytical procedures, and appropriate acceptance criteria, which are numerical limits, ranges, or other criteria for the tests described. It establishes the set of criteria to which a drug substance or drug product should conform to be considered acceptable for its intended use. "Conformance to specifications" means that the drug substance and / or drug product, when tested according to the listed analytical procedures, will meet the listed acceptance criteria. Specifications are critical quality standards that are proposed and justified by the manufacturer and approved by regulatory authorities as conditions of approval. The specifications imposed in our lab and coming from two years of repeated synthesis are presented in Table 2. On the one hand, classical

characterization focuses on the Surface Plasmon Resonance (SPR) measurement (λ_{max}), the hydrodynamic diameter (Dh) and ζ potential determination. SPR is directly linked to NP size, shape, core/corona composition and suspension medium(Vilela *et al.*, 2012). Dh takes into consideration the gold core size plus surface chemistry and some hydration layers. ζ potential somehow reflects ion capping AuNP surface (*i.e.* citrate ions). On the other hand, CZE coupled to DAD leads to μ_{EP} which is directly linked to the three parameters described above. As a separation method, it also allows calculating the content percentage (assay on the main product) in each batch and is therefore highly complementary to classical approaches. Therefore, each newly synthesized AuNP-Cit batch that did not reach specifications described below was automatically discarded.

Table 2: Quality specifications defined for citrate stabilized AuNP, assay % refers to the main product content.

Specifications	UV-vis/DLS/electrophoresis coupled to DLS			CZE		
	λ_{max} (nm)	Dh (nm)	ζ (mV)	μ_{EP} (× 10^{-4} $cm^2.V^{-1}.s^{-1}$)	λ_{max} (nm)	Assay (%)
AuNP-Cit	514 ± 1	6.5 ± 0.9	-32.6 ± 0.7	-1.75 ± 0.44	521 ± 3	> 86.0

More than 31 independent batches with the same synthesis process were analyzed and confronted to those specifications. Four parameters (λ_{max}, Dh, ζ potential, μ_{EP}) are presented in Figure 2 as an example of control card obtained through the batch-to-batch survey. Horizontal plain lines represented the specification limits of each parameter. Among the 31 batches, 9 of them were out of specifications right after synthesis. Respectively, λ_{max}, Dh, ζ and CZE found 16 % (5 on 31), 13 % (4 on 31), 19 % (6 on 31) and 29 % (9 on 31) batches to be out of conformity. This indicated that 3 out of 9 non-conform batches were only detected using CZE (batches 16, 18 and 25) indicating that classical methods may not be sufficient to determine AuNP conformity or long-term stability.

For each batch, the content percentage was calculated (Table 2). In absence of any certificate standard with known purity, in a first approximation and to compare the different batches, the assay corresponding to the

main product percentage was determined by a classic normalization process (corrected area of the main peak *versus* the sum of all other peaks corrected area). According to ICH Q2(R1) recommendations (ICH-Q2(R1)) the limit of detection (LOD) was calculated as a Signal-to-Noise Ratio equal to 3. This LOD value represented 2.6 ± 0.5 % of the AuNP-Cit main peak. For all the 31 batches analyzed, the assay percentage was above the 86.0 % specification (data not shown). However, impurities were present. They may originate from either raw material and/or degradation products: uncapped or unfunctionalized gold core responsible for AuNP aggregation and non-homogeneous surface. Only neutral impurities were detected on the electrophoregrams. After synthesis, these impurities represented 2.7 ± 1.3 % of the synthesized AuNP-Cit (mean of the 31 different batches).

After developing quality control on our own AuNP-Cit, AuNP from other laboratories of Or Nano network (GDR-Or-Nano) were tested. The three first batches to be tested were AuNP-Cit of different sizes. All three batches (E, F and G) were received with some parameters being already measured (λ_{max} and Dh mainly, Table 3). These parameters were compared to our own results. λ_{max} were similar, on the contrary Dh values differed but this parameter is very dependent on the laser wavelength used (and also on other parameters such salt concentration, measurement duration, etc.). As batch E was received in very low volume from another laboratory, a complete evaluation comprising Dh and ζ potential measurements could not been performed.

A typical electrophoregram is presented in Figure 3. Detection was performed from 200 to 600 nm in order to monitor in the same experiment: possible different AuNP population (Surface Plasmon Band, around 520 nm) and organic impurity profile (at 214 nm). For batches E, F and G, only one peak was present at 214 and 520 nm. This indicated the presence of a single AuNP population and the absence of organic impurity. CZE is an interesting tool helping to visualize the purity of newly synthetized batch and can be applied to different types of AuNP-Cit (size from 5 nm to 40 nm).

Table 3: Comparison between announced and controlled characteristics of lab-made AuNP-Cit. Announced concentrations were determined by UV-Vis spectrophotometric measurements and controlled ones using HPLC coupled to a UV-Vis detector.

Announced Characteristics					Controlled Characteristics				
Batch	λ_{max} (nm)	Dh (nm)	ζ (mV)	Concentration (mM)	λ_{max} (nm)	Dh (nm)	ζ (mV)	Assay (%)	Concentration (mM)
E	524 ± 2	9.5 ± 1.8	N.D.	5.7 ± 0.5	523 ± 1	N.D.	N.D.	100.0 ± 2.5	5.3 ± 0.2
F	516 ± 1	21.5 ± 2.7	N.D.	7.4 ± 0.7	516 ± 1	5.0 ± 1.0	-24.2 ± 3.1	100.0 ± 2.5	5.2 ± 1.1
G	519 ± 1	34.0 ± 2.9	N.D.	10.6 ± 0.4	519 ± 2	38.8 ± 3.8	-52.3 ± 4.6	100.0 2.5	7.0 ± 0.9

N.D.: Not determined

As synthesis of AuNP usually requires several purification steps to obtain the final product (Alric *et al.*, 2013; Gilles *et al.*, 2014) , the impact of purification steps using CZE was monitored.

First, purification of AuNP-Cit (batch E) was investigated: electrophoregrams went from a complicated one with several peaks for raw suspension (Figure 4A) to a very pure one, showing only one AuNP population with no detected impurity in CZE after three cycles of ultracentrifugation (Figure 4B). We then evaluated our method with more complex AuNP: AuNP@DTDTPA. This synthesis implied steps of solvent removal and filtration. AuNP@DTDTPA are designed for combining medical imaging (X-ray imaging owing to the gold core, magnetic resonance imaging (MRI) and nuclear imaging after immobilization of gadolinium ions or radioisotopes in the DTDTPA shell, respectively) and for radiosensitization (Alric *et al.*, 2013; Alric *et al.*, 2008; Arifin *et al.*, 2011). As demonstrated by previous *in vivo* experiments, AuNP@DTDTPA exhibit a high potential for MRI-guided radiotherapy (Butterworth *et al.*, 2016; Miladi *et al.*, 2014). Although extensive characterization of AuNP@DTDTPA has to be performed prior to *in vivo* administration, for this purpose, CZE could be of interest as it would provide crucial information about the quality grade of the suspension of theranostic nanoparticles before intravenous injection. Two different samples of AuNP@DTDTPA were analyzed. The first one was the raw suspension (AuNP@DTDTPA in aqueous sodium hydroxide solution at pH 8) which was prepared from a black powder obtained after filtration of the reaction mixture and rinsing the retentate successively with HCl,

water and acetone. The second was prepared as for intravenous injection from the raw suspension which was used as starting material but with a final purification step. The resulting electrophoregrams are shown in Figures 4C and 4D.

Before purification (Figure 4A) the sample presented 9 different peaks at 214 nm. The main one (peak n°8) was set with a relative migration time (RMT) of 1 (Table 4). Among those 9 peaks, 5 of them (peaks n°1, 3, 5, 6 and 8) were AuNP populations due to their absorbance at 520 nm. Purities were calculated by dividing the corrected area (CA) of the main peak by the sum of all other peak at the same wavelength. The sample presented a purity of 45.7 % considering the total impurity values (214 nm) or 32.6 % considering only nanoparticle populations (520 nm). Interestingly, sample purity was found lower at 520 nm than at 214 nm. This was caused by the presence of peak n°6. Its CA was even higher than the one of the main peak, indicating that there were two major AuNP populations coexisting in the same sample. Those two populations were not detected through classical methods. DLS values of unpurified sample gave uncoherent values (Dh = 216.1 nm) certainly caused by a relatively important number of aggregates and impurities among the suspension.

Table 4: Impurity profile of AuNP@DTDTPA by CZE analyzes after synthesis (Raw) and after purification steps (purified). The line in grey represents the main AuNP peak. RMT : Relative Migration Time; CA : corrected area

	AuNP@DTDTPA raw				AuNP@DTDTPA purified			
	214 nm		**520 nm**		**214 nm**		**520 nm**	
Peak	**RMT**	**CA**	**RMT**	**CA**	**RMT**	**CA**	**RMT**	**CA**
1	0.38	3490	0.38	647				
2	0.39	3103						
3	0.41	23412	0.41	5378				
4	0.59	43008						
5	0.65	6730	0.65	1013	0.63	13220		
6	0.71	95419	0.70	15647	0.73	28861	0.73	12847

7	0.95	678						
8	1.00	148070	1.00	10989	1.00	453025	1.00	67636
9	1.93	342			1.91	6289		

After purification only four peaks remained (Figure 4B). Two of them (peaks n°5 and 9) were attributed to organic impurities with no absorption at 520 nm. The other two peaks (peaks n°6 and 8) corresponded to two different AuNP populations. This led to a sample total purity of 90.4 % (normalized to the main peak at 214 nm) or a nanoparticle purity of 84.0 % (normalized to the main peak at 520 nm). Purity was respectively increased by 2.0 and 2.6 times through purification steps. CZE successfully assess the purity of a complex AuNP sample whereas classical methods give only hints of a single AuNP population. After purification steps, Dh of AuNP@DTDTPA was in accordance with expected values (9.1 nm) with a surface charge of -37.6 mV. However, these values were global results that prove neither the co-existence of several NP populations in the same sample, nor the presence of impurities.

In the end, in the presence of complex samples (in terms of populations/impurities), CZE proved its capacity to discriminate a mix of AuNP populations and showed the benefits of purification steps on two different AuNP in terms of size and chemical stabilization.

3.2. AuNP-Cit stability monitoring

Once purified and characterized, crucial questions about AuNP remains their stability and the long-term storage. A previous study has shown that AuNP-Cit remained stable for no more less than 20 days (Pallotta *et al.*, 2016). This study was based only on 3 batches. Thus, this issue was more carefully addressed with 18 independent batches which were fully characterized just after synthesis (D0) and after 20 days (D20) of storage. Results are shown in Table 5.

Table 5: Physicochemical characterization of AuNP-Cit using classical approaches and CZE after synthesis (Day 0) and 20 days of storage (Day 20). Values out of specifications after 20 days are marked in grey. Batch numbers correspond to the same batches than presented in Figure 2.

	Day 0					Day 20				
	λ_{max} (nm)	Dh (nm)	ζ (mV)	μ_{EP} ($\times 10^{-4}$ $cm^2.V^{-1}.s^{-1}$)	λ_{max} (nm)	λ_{max} (nm)	Dh (nm)	ζ (mV)	μ_{EP} ($\times 10^{-4}$ $cm^2.V^{-1}.s^{-1}$)	λ_{max} (nm)
Specifications	**514 ± 1**	**6.5 ± 0.9**	**-32.6 ± 0.7**	**-1.75 ± 0.44**	**521 ± 3**	**514 ± 1**	**6.5 ± 0.9**	**-32.6 ± 0.7**	**-1.75 ± 0.44**	**521 ± 3**
Batch number										
8	513	6,3	-32,9	-1,90	522	514	6,6	-16,2	-1,11	526
9	513	6,0	-31,9	-1,53	520	515	6,5	-13,9	-0,92	528
10	513	5,9	-31,9	-1,73	520	516	7,9	-29,8	-2,68	520
11	513	6,3	-32,8	-1,46	522	513	6,8	-32,4	-2,14	522
12	513	5,9	-32,3	-1,52	520	513	6,7	-32,9	-4,71	514
13	513	5,6	-33,1	-1,82	524	514	6,7	-32,9	-2,19	518
14	513	6,2	-33,3	-1,71	519	516	15,6	-9,7	-0,51	524
15	513	5,6	-33,2	-1,63	524	515	6,2	-32,5	-0,69	524
19	514	6,9	-32,7	-1,75	518	514	6,9	-32,8	-1,32	518
20	514	6,7	-32,4	-1,75	516	514	5,7	-32,9	-2,38	520
22	514	6,7	-32,1	-1,96	519	514	5,6	-33,1	-2,54	528
23	513	6,7	-33,2	-1,55	514	515	6,9	-33,1	-2,23	532
26	514	6,8	-32,4	-1,64	520	514	6,6	-16	-1,01	526
27	514	6,9	-32,7	-1,73	523	516	7,5	-13,6	-0,88	528
28	514	5,9	-31,9	-1,33	521	517	7,9	-29,8	-1,28	520
29	515	6,7	-32,0	-1,34	519	513	6,8	-32,4	-2,14	522
30	514	7,1	-32,8	-2,18	520	514	7,4	-32,3	-4,71	514
31	514	7,0	-33,2	-1,61	518	515	6,8	-32,9	-1,29	520

Considering results from both approaches (classical or CZE) at D20, almost 72 % of batches (13 out of 18) were out of the specifications, indicating the degradation of AuNP-Cit suspensions. However, when classical methods are compared, only 22 % of batches (4 out of 18) are discarded considering only λ_{max} or Dh monitoring and 39 % (7 out of 18) through ζ potential measurement. While every batch discarded by classical methods is confirmed by CZE, 6 batches are only excluded using this methodology. These results confirmed the observations made in part 3.1 and show that CZE is a more powerful tool to monitor the stability of AuNP

samples. Thus, if one wants to establish a gradation of the parameters in their capacity to analyze and discriminate AuNP batches according to specifications, the more powerful would be CZE, followed by ζ potential measurement, λmax and Dh being the least indicative of the AuNP colloidal state.

3.3. Commercial batches analysis

Considering results obtained in part 3.2 in terms of stability or impurities, one could be skeptical about commercial AuNP-Cit. Commercially available AuNP-Cit are sold with a certificate of analysis. At best, it gives information on size (gold core or Dh), polydispersity, number of particles per mL, surface charge … all of this being obtained through classical methods and often a stability indication (up to 1 year in some cases). But the overall quality of AuNP is never evaluated. Indeed, as AuNP are not considered as active pharmaceutical ingredients, there is no impurity limit or stability requirements. Four commercially available AuNP-Cit batches were analyzed, under a single-blinded randomized trial, using both approaches described previously and results were compared to the provider's certificate of analysis.

Most of our results (Table 6) were in accordance with reported values on the certificate of analysis (ζ potentials for Batches #1 to #4 were not reported by suppliers).

Table 6: Comparison of the characterization of commercially available AuNP-Cit by classical methods with the data from the provider.

Commercial batch number	Results provenance	Core size (nm)	Dh (nm)	ζ potential (mV)	λ_{max} (nm)
#1	Provider	5	19	N.R.	521
	This study	5	13	-34.5	521
#2	Provider	5	19	N.R.	519
	This study	5	7	-33.1	516
#3	Provider	5.0 ± 0.6	N.R.	N.R.	516
	This study	5.0 ± 0.7	7	-29.3	515
#4	Provider	5.0 ± 0.6	N.R.	N.R.	515
	This study	5.0 ± 2.0	7	-19.7	514

N.R.: Not Reported

In parallel, these 4 batches were analyzed by CZE. The assay percentage, total organic impurities (at 214 nm) and nanoparticular impurities (other AuNP population at 520 nm) are presented in Table 7. Except for Batch #3 that presented a purity superior to 90 % with no other AuNP population, the other 3 batches displayed purity profiles inferior to 80 %. The low purity (76.8 %) of Batch #2 was only caused by a high organic impurity level (23.2 %). CZE electrophoregrams showed the presence of 3 distinct peaks at 214 nm. Those organic impurities probably derived from the synthesis.

For the 2 batches left (#1 and #4), impurity profiles were composed of both organic and nanoparticular impurities. Batch #1 electrophoregrams were composed of 4 organic impurities and 2 other AuNP populations. The same profile was found for Batch #4 (3 organic and 1 AuNP populations). Those AuNP populations could derive directly from a synthesis with an incomplete reaction or indicate of a loss of stability of the AuNP suspension forming aggregates. As these populations are present at low concentrations, classical methods do not detect them.

Table 7: CZE analyzes of commercial AuNP-Cit.

Commercial batch number	Assay (%)	Organic impurities (%)	Nanoparticular impurities (%)
#1	79.8	6.1	14.1
#2	76.8	23.2	0.0
#3	90.5	9.5	0.0
#4	68.3	11.6	20.1

Those results raised some questions concerning the quality of commercially AuNP. In the worst cases, up to 30 % of the sample was composed of AuNP different of the one expected (in terms of size, surface charge, surface chemistry …). One serious problem is the stability of suspensions. When buying AuNP, a large delay between synthesis and purchase usually occurs. In that case, characterizations made on the synthesis day can be different from the one performed at reception. If new AuNP populations are formed (as in Batches #1 and #3),

their impact on experiments can affect the obtained results, leading to a lack of reproducibility or misinterpretation of results (reactivity, catalysis, functionalization, biological evaluation, …).

4. Conclusion

The more and more important use of nanoparticles as new therapeutic tools, considering the limited knowledge on their human toxicity, requires a strict control of them. As with other "conventional" drugs, all nano-objects should be submitted to a strictly control before use. In this paper, we showed the major interest of using a separation method (CZE) for evaluating AuNP quality. In the highly controlled pharmaceutical field, marketed products go through a relatively long regulatory process to secure their use and have to prove their added value in relation to what already exists on the market. For each pharmaceutical raw material (called ingredients), there is a specific monograph. This one establishes its exact definition (*i.e.* its identification), evaluates its quality including purity and limitation of impurities. However, to date, there is not any specific monograph for nanoparticles. Faced with their increasing use for pharmaceutical purposes, it seemed urgent and necessary to have nano-objects of utterly defined quality and meeting international standards and procedures that yet remains to be defined.

Acknowledgments:

The authors thank Sayens (SATT French network) and Incubateur Lorrain for their financial supports and the GDR Or-Nano for its scientific support. The authors are grateful to Pr A. Le Faou for improving the English of the manuscript.

The present work has benefited from the CYTOMETRY / ELECTRONIC MICROSCOPY / LIGHT MICROSCOPY facility of Imagerie-Gif, (http://www.i2bc.paris-saclay.fr), member of IBiSA (http://www.ibisa.net), supported by “France-BioImaging” (ANR-10-INBS-04-01), and the Labex “Saclay Plant Sciences” (ANR-10-LABX-0040-SPS).

References

Aldewachi, H., Chalati, T., Woodroofe, M. N., Bricklebank, N., Sharrack, B., and Gardiner, P., 2017. Gold nanoparticle-based colorimetric biosensors, Nanoscale 10, 18-33.

Alric, C., Miladi, I., Kryza, D., Taleb, J., Lux, F., Bazzi, R., Billotey, C., Janier, M., Perriat, P., Roux, S., and Tillement, O., 2013. The biodistribution of gold nanoparticles designed for renal clearance, Nanoscale 5, 5930-9.

Alric, C., Taleb, J., Le Duc, G., Mandon, C., Billotey, C., Le Meur-Herland, A., Brochard, T., Vocanson, F., Janier, M., Perriat, P., Roux, S., and Tillement, O., 2008. Gadolinium chelate coated gold nanoparticles as contrast agents for both X-ray computed tomography and magnetic resonance imaging, Journal of the American Chemical Society 130, 5908-15.

Arifin, D. R., Long, C. M., Gilad, A. A., Alric, C., Roux, S., Tillement, O., Link, T. W., Arepally, A., and Bulte, J. W., 2011. Trimodal gadolinium-gold microcapsules containing pancreatic islet cells restore normoglycemia in diabetic mice and can be tracked by using US, CT, and positive-contrast MR imaging, Radiology 260, 790-8.

Bhattacharjee, S., 2016. DLS and zeta potential - What they are and what they are not?, J Control Release 235, 337-51.

Brigger, I., Dubernet, C., and Couvreur, P., 2002. Nanoparticles in cancer therapy and diagnosis, Adv Drug Deliv Rev 54, 631-51.

Butterworth, K. T., Nicol, J. R., Ghita, M., Rosa, S., Chaudhary, P., McGarry, C. K., McCarthy, H. O., Jimenez-Sanchez, G., Bazzi, R., Roux, S., Tillement, O., Coulter, J. A., and Prise, K. M., 2016. Preclinical evaluation of gold-DTDTPA nanoparticles as theranostic agents in prostate cancer radiotherapy, Nanomedicine (Lond) 11, 2035-47.

Clogston, J.D., Crist, R.M., McNeil, S.E., Vauthier, C., and Ponchel, G., 2016. Polymer Nanoparticles for Nanomedicines: A Guide for their Design, Preparation and Development, Springer International Publishing, 187-203.

Coty, J. B., and Vauthier, C., 2018. Characterization of nanomedicines: A reflection on a field under construction needed for clinical translation success, J Control Release 275, 254-68.

D'Mello, S. R., Cruz, C. N., Chen, M. L., Kapoor, M., Lee, S. L., and Tyner, K. M., 2017. The evolving landscape of drug products containing nanomaterials in the United States, Nat Nanotechnol 12, 523-29.

Devi, R. V., Doble, M., and Verma, R. S., 2015. Nanomaterials for early detection of cancer biomarker with special emphasis on gold nanoparticles in immunoassays/sensors, Biosens Bioelectron 68, 688-98.

Duesberg, G. S., Muster, J., Krstic, V., Burghard, M., and Roth, S., 1998. Chromatographic size separation of single-wall carbon nanotubes, Applied Physics A 67, 117-19.

Franze, B., Strenge, I., and Engelhard, C., 2017. Separation and detection of gold nanoparticles with capillary electrophoresis and ICP-MS in single particle mode (CE-SP-ICP-MS), Journal of Analytical Atomic Spectrometry 32, 1481-89.

GDR-Or-Nano, http://or-nano.insp.upmc.fr.

Gilles, M., Brun, E., and Sicard-Roselli, C., 2014. Gold nanoparticles functionalization notably decreases radiosensitization through hydroxyl radical production under ionizing radiation, Colloids and Surfaces B: Biointerfaces 123, 770-77.

Gioria, S., Caputo, F., Urban, P., Maguire, C. M., Bremer-Hoffmann, S., Prina-Mello, A., Calzolai, L., and Mehn, D., 2018. Are existing standard methods suitable for the evaluation of nanomedicines: some case studies, Nanomedicine (Lond) 13, 539-54.

Gonzalez-Fuenzalida, R. A., Moliner-Martinez, Y., Molins-Legua, C., and Campins-Falco, P., 2019. Miniaturized liquid chromatography coupled on-line to in-tube solid-phase microextraction for characterization of metallic nanoparticles using plasmonic measurements. A tutorial, Anal Chim Acta 1045, 23-41.

Guo, J., Rahme, K., He, Y., Li, L. L., Holmes, J. D., and O'Driscoll, C. M., 2017. Gold nanoparticles enlighten the future of cancer theranostics, Int J Nanomedicine 12, 6131-52.

Halamoda-Kenzaoui, Blanka, Holzwarth, Uwe, Roebben, Gert, Bogni, Alessia, and Bremer-Hoffmann, Susanne, 2019. Mapping of the available standards against the regulatory needs for nanomedicines, Wiley Interdisciplinary Reviews: Nanomedicine and Nanobiotechnology 11, e1531.

Hardie, J., Jiang, Y., Tetrault, E. R., Ghazi, P. C., Tonga, G. Y., Farkas, M. E., and Rotello, V. M., 2016. Simultaneous cytosolic delivery of a chemotherapeutic and siRNA using nanoparticle-stabilized nanocapsules, Nanotechnology 27, 374001.

ICH-Q1A(R2), Stability Testing of New Drug Substances and Products.

ICH-Q2(R1), Note for Guidance on Validation of Analytical Procedures : Text and Methodology. Ref. CPMP/ICH/381/95.

ICH-Q3A(R2), Impurities in New Drug Substances.

ICH-Q6A, Specifications: Test Procedures and Acceptance Criteria for New Drug Substances and New Drug Products: Chemical Substances.

ISO-22412:2017, 2017. Particle Size Analysis - Dynamic Light Scattering (DLS), ISO.

ISO/TR-18196:2016, 2016. Nanotechnologies - Measurements Technique Matrix for the Characterization of Nano-Objects, ISO.

ISO/TS, 2008. Nanotechnologies - Terminology and definitions for nano-objects, nanoparticle, nanofibre and nanoplate.

Lu, F., Doane, T.L., Zhu, J.J., and Burda, C., 2012. Gold nanoparticles for diagnostic sensing and therapy, Inorganica Chimica Acta 393, 142-53.

Miladi, I., Alric, C., Dufort, S., Mowat, P., Dutour, A., Mandon, C., Laurent, G., Brauer-Krisch, E., Herath, N., Coll, J. L., Dutreix, M., Lux, F., Bazzi, R., Billotey, C., Janier, M., Perriat, P., Le Duc, G., Roux, S., and Tillement, O., 2014. The in vivo radiosensitizing effect of gold nanoparticles based MRI contrast agents, Small 10, 1116-24.

Mishra, G., and Mukhopadhyay, M., 2019. TiO2 decorated functionalized halloysite nanotubes (TiO2@HNTs) and photocatalytic PVC membranes synthesis, characterization and its application in water treatment, Scientific Reports 9, 4345.

Muneshwar, T., and Cadien, K., 2018. Comparing XPS on bare and capped ZrN films grown by plasma enhanced ALD: Effect of ambient oxidation, Applied Surface Science 435, 367-76.

Nie, L., Liu, F., Ma, P., and Xiao, X., 2014. Applications of gold nanoparticles in optical biosensors, J Biomed Nanotechnol 10, 2700-21.

Pallotta, A., Boudier, A., Leroy, P., and Clarot, I., 2016. Characterization and stability of gold nanoparticles depending on their surface chemistry: Contribution of capillary zone electrophoresis to a quality control, Journal of Chromatography A 1461, 179-84.

Pallotta, A., Clarot, I., Sobocinski, J., Fattal, E, and Boudier, A., 2019. Nanotechnologies for Medical Devices: Potentialities and Risks, ACS Applied Bio Materials 2, 1-13.

Pallotta, A., Philippe, V., Boudier, A., Leroy, P., and Clarot, I., 2018. Highly sensitive and simple liquid chromatography assay with ion-pairing extraction and visible detection for quantification of gold from nanoparticles, Talanta 179, 307-11.
Rawal, S., and Patel, M. M., 2019. Threatening cancer with nanoparticle aided combination oncotherapy, J Control Release 301, 76-109.
Shawky, S. M., Awad, A. M., Allam, W., Alkordi, M. H., and El-Khamisy, S. F., 2017. Gold aggregating gold: A novel nanoparticle biosensor approach for the direct quantification of hepatitis C virus RNA in clinical samples, Biosens Bioelectron 92, 349-56.
Silva, C. O., Pinho, J. O., Lopes, J. M., Almeida, A. J., Gaspar, M. M., and Reis, C., 2019. Current Trends in Cancer Nanotheranostics: Metallic, Polymeric, and Lipid-Based Systems, Pharmaceutics 11.
Singh, M., Harris-Birtill, D. C., Markar, S. R., Hanna, G. B., and Elson, D. S., 2015. Application of gold nanoparticles for gastrointestinal cancer theranostics: A systematic review, Nanomedicine 11, 2083-98.
Slot, J. W., and Geuze, H. J., 1981. Sizing of protein A-colloidal gold probes for immunoelectron microscopy, J Cell Biol 90, 533-6.
Stavis, S. M., Fagan, J. A., Stopa, M., and Liddle, J. A., 2018. Nanoparticle Manufacturing – Heterogeneity through Processes to Products, ACS Applied Nano Materials 1, 4358-85.
Stewart, P. L., 2017. Cryo-electron microscopy and cryo-electron tomography of nanoparticles, Wiley Interdiscip Rev Nanomed Nanobiotechnol 9.
Surugau, N., and Urban, P. L., 2009. Electrophoretic methods for separation of nanoparticles, J Sep Sci 32, 1889-906.
Tournebize, J., Boudier, A., Joubert, O., Eidi, H., Bartosz, G., Maincent, P., Leroy, P., and Sapin-Minet, A., 2012. Impact of gold nanoparticle coating on redox homeostasis, International Journal of Pharmaceutics 438, 107-16.
Tournebize, J., Boudier, A., Sapin-Minet, A., Maincent, P., Leroy, P., and Schneider, R., 2012. Role of gold nanoparticles capping density on stability and surface reactivity to design drug delivery platforms, ACS Appl Mater Interfaces 4, 5790-9.
Tournebize, J., Sapin-Minet, A., Schneider, R., Boudier, A., Maincent, P., and Leroy, P., 2011. Simple spectrophotocolorimetric method for quantitative determination of gold in nanoparticles, Talanta 83, 1780-3.
Varenne, F., Botton, J., Merlet, C., Vachon, J.-J., Geiger, S., Infante, I. C., Chehimi, M. M., and Vauthier, C., 2015. Standardization and validation of a protocol of zeta potential measurements by electrophoretic light scattering for nanomaterial characterization, Colloids and Surfaces A: Physicochemical and Engineering Aspects 486, 218-31.
Varenne, F., Makky, A., Gaucher-Delmas, M., Violleau, F., and Vauthier, C., 2016. Multimodal Dispersion of Nanoparticles: A Comprehensive Evaluation of Size Distribution with 9 Size Measurement Methods, Pharm Res 33, 1220-34.
Vilela, D., Gonzalez, M. C., and Escarpa, A., 2012. Sensing colorimetric approaches based on gold and silver nanoparticles aggregation: chemical creativity behind the assay. A review, Anal Chim Acta 751, 24-43.
Xia, H., Xiahou, Y., Zhang, P., Ding, W., and Wang, D., 2016. Revitalizing the Frens Method To Synthesize Uniform, Quasi-Spherical Gold Nanoparticles with Deliberately Regulated Sizes from 2 to 330 nm, Langmuir 32, 5870-80.
Yi, Y., Kim, H. J., Mi, P., Zheng, M., Takemoto, H., Toh, K., Kim, B. S., Hayashi, K., Naito, M., Matsumoto, Y., Miyata, K., and Kataoka, K., 2016. Targeted systemic delivery of siRNA to cervical cancer model using cyclic RGD-installed unimer polyion complex-assembled gold nanoparticles, J Control Release 244, 247-56.
Zattoni, A., Rambaldi, D. C., Reschiglian, P., Melucci, M., Krol, S., Garcia, A. M. C., Sanz-Medel, A., Roessner, D., and Johann, C., 2009. Asymmetrical flow field-flow fractionation with multi-angle light scattering detection for the analysis of structured nanoparticles, Journal of Chromatography A 1216, 9106-12.

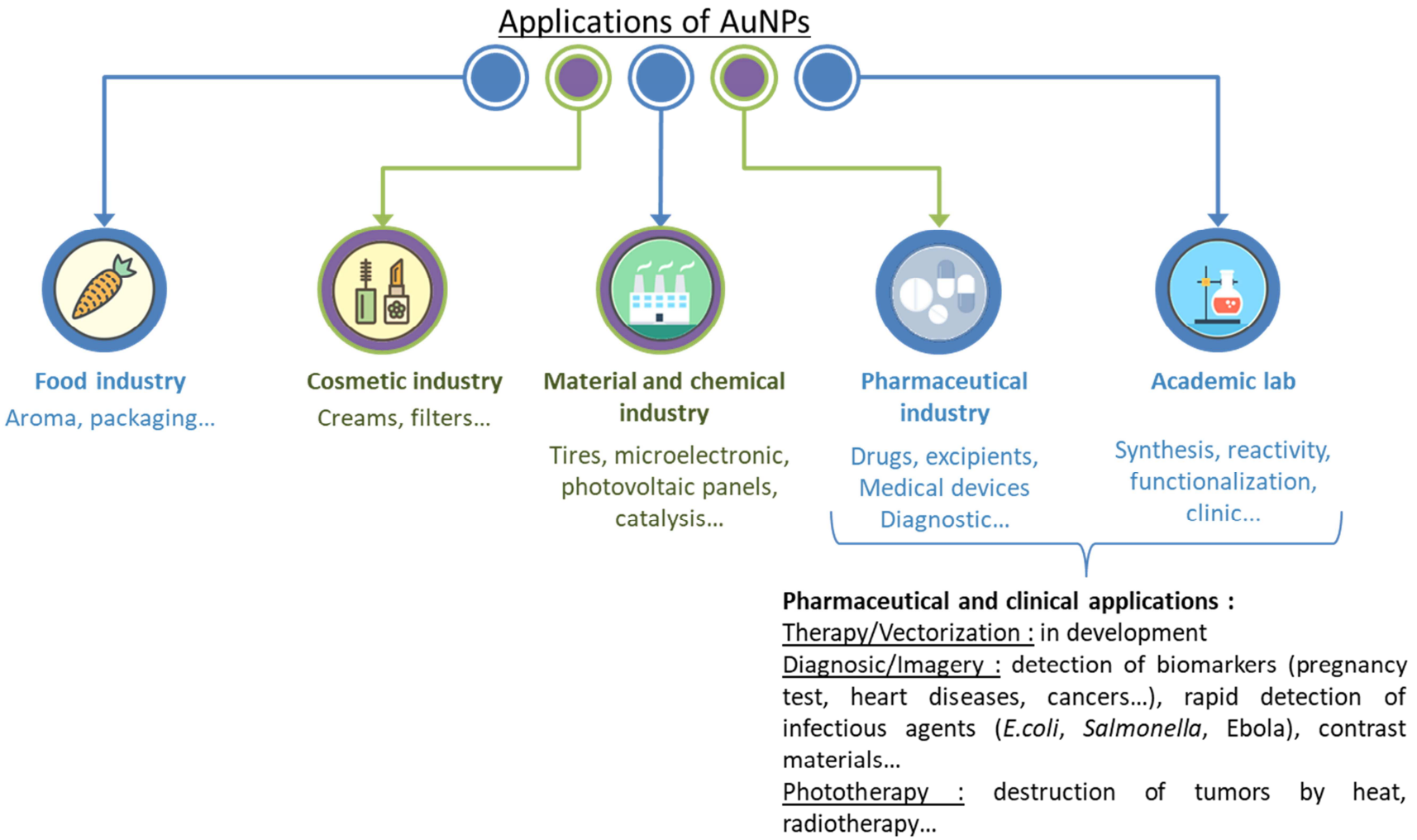
Applications of AuNPs
Food industry
Aroma, packaging…
Cosmetic industry
Creams, filters…
Material and chemical industry
Tires, microelectronic, photovoltaic panels, catalysis…
Pharmaceutical industry
Drugs, excipients, Medical devices Diagnostic…
Academic lab
Synthesis, reactivity, functionalization, clinic…
Pharmaceutical and clinical applications :
Therapy/Vectorization : in development
Diagnosic/Imagery : detection of biomarkers (pregnancy test, heart diseases, cancers…), rapid detection of infectious agents (E.coli, Salmonella, Ebola), contrast materials…
Phototherapy : destruction of tumors by heat, radiotherapy…

Figure 1

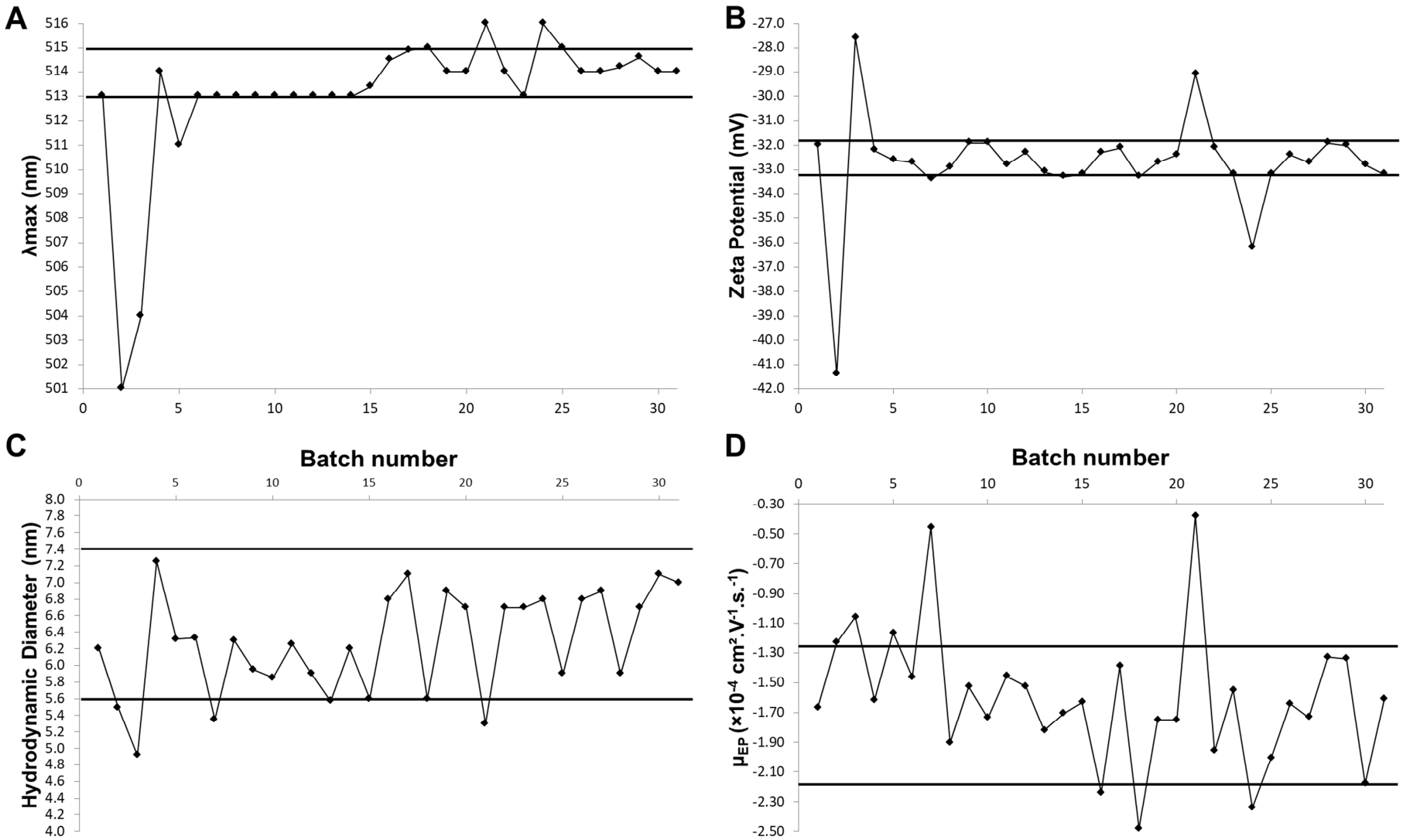
A
λmax (nm)
B
Zeta Potential (mV)
C
Hydrodynamic Diameter (nm)
Batch number
D
Batch number
μ_{EP} (×10^{-4} cm^2.V^{-1}.s.$^{-1}$)

Figure 2

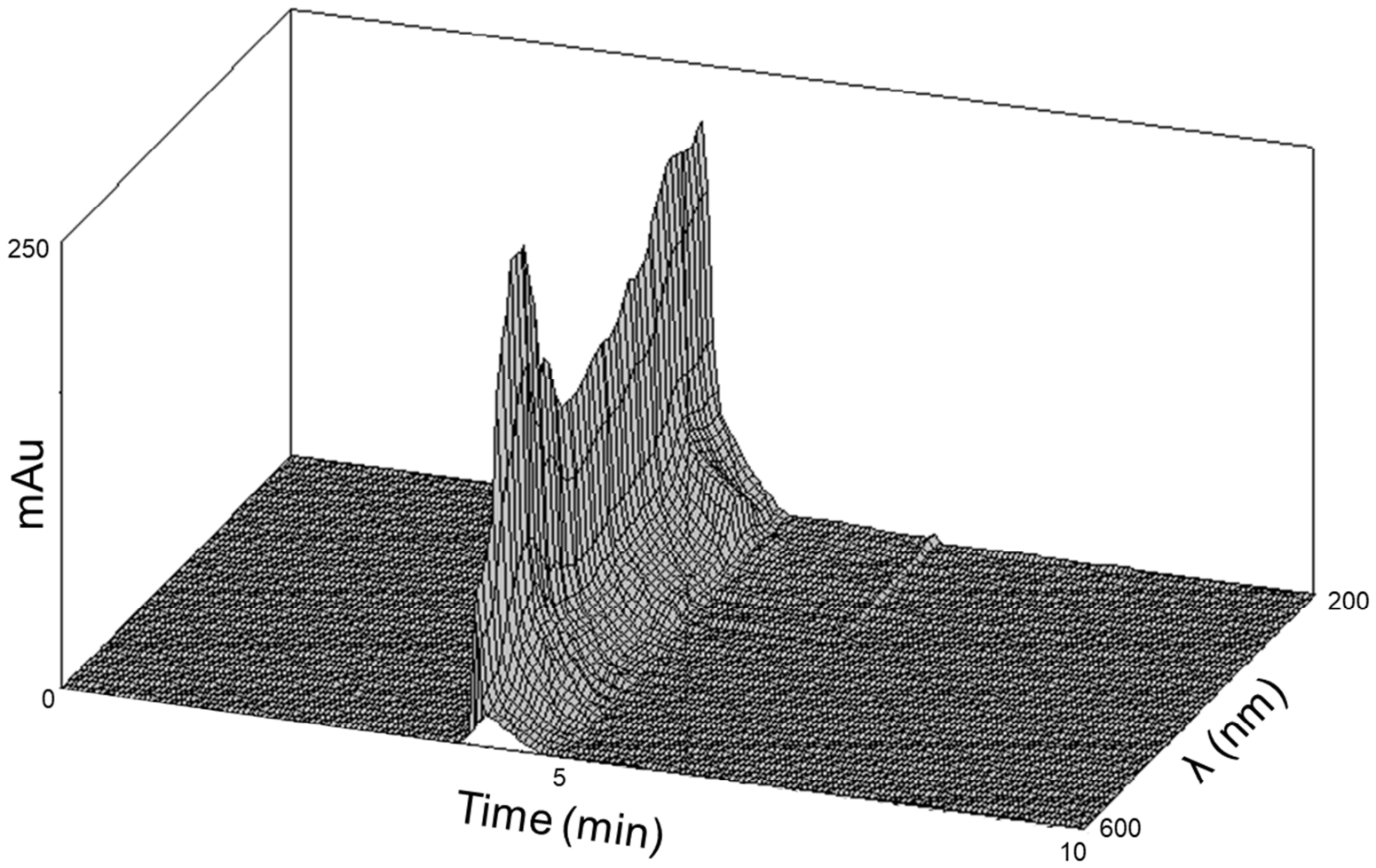

Figure 3

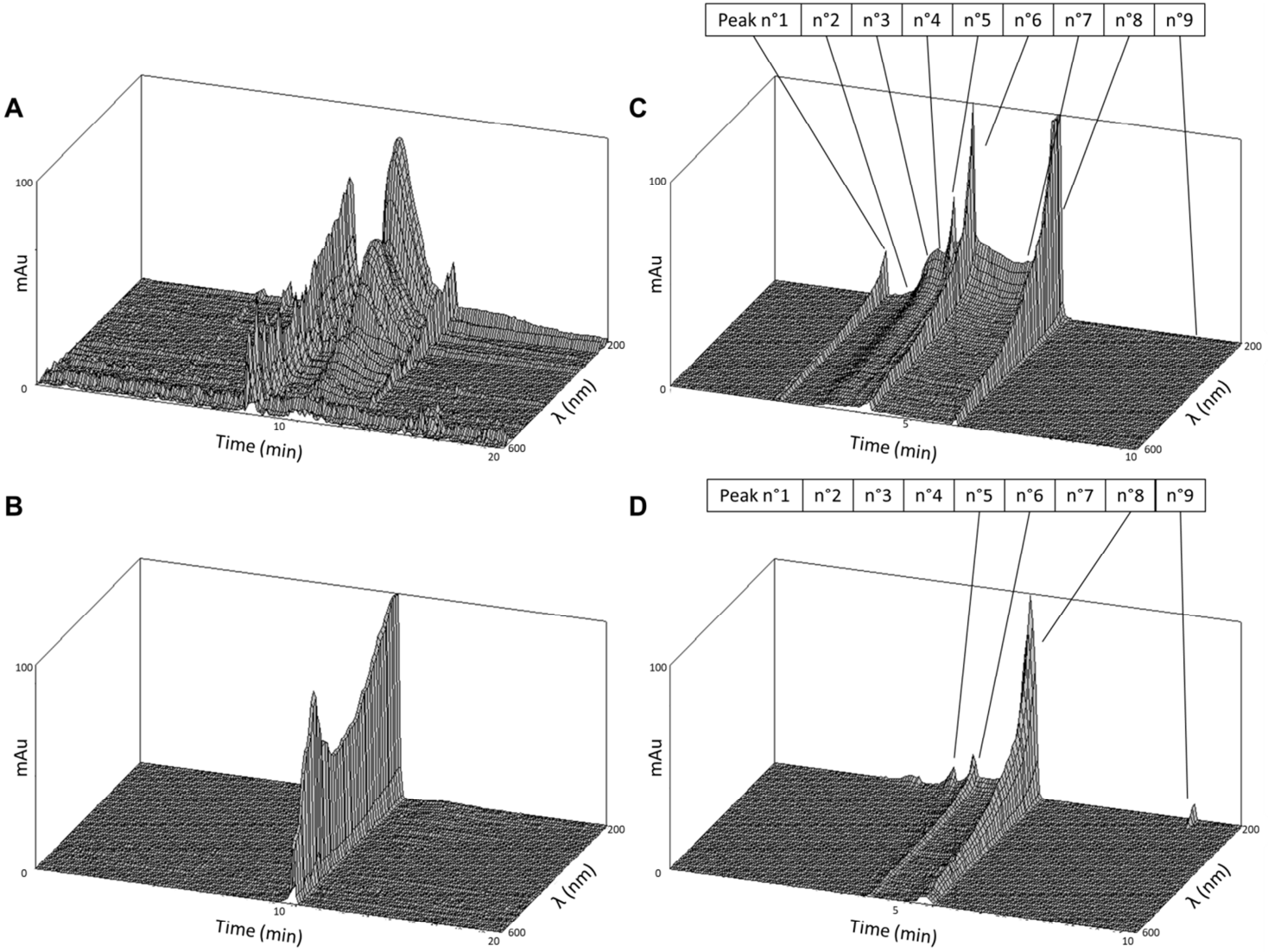
A
B
C
D
Peak n°1
n°2
n°3
n°4
n°5
n°6
n°7
n°8
n°9
mAu
100
0
Time (min)
10
20
5
λ (nm)
200
600

Figure 4

NP Synthesis
Batch 1
Batch 2
Batch 3
Batch 4
Batch 5...
Quality Control
Batch Release
Discarded
Discarded
Discarded
Stability assessment
Classical evaluation
Versus
Capillary Zone Electrophoresis evaluation